PERGAMON

International Journal of Solids and Structures 40 (2003) 5051–5061

INTERNATIONAL JOURNAL OF SOLIDS and STRUCTURES

www.elsevier.com/locate/ijsolstr

Properties of equal bodies in contact with friction

J. Jäger

Lauterbach Verfahrenstechnik, Blattwiesenstrasse 7, D-76227 Karlsruhe, Germany

Received 24 August 2002; received in revised form 20 January 2003

Abstract

The properties of a reduced friction model for elastic bodies with general surfaces in contact are explained, and it is proved that the tangential friction problem can be reduced to the normal problem. The tangential solution results as the difference of the full slip traction for actual contact and a smaller contact area, which represents the stick area (or multiple areas). The local traction in the slip area opposes the relative motion in the same way as the normal relative approach opposes the contact pressure, as required by Coulomb's slip inequality. The stick inequality for the traction is identical with the contact condition of positive pressure. A superposition method for general loading scenarios is explained and an example is calculated at the end. The force displacement relation of the reduced friction model agrees well with the FEM solution, even for dissimilar materials, because the dissimilarity effect is small in practical applications. Since numerical solutions of frictional contact are rare in literature, an example for a contact area with a hole is presented.

Keywords: Friction; Elastic; Traction

1. Introduction

Contact problems are a field of increasing importance in mechanics. Typical applications are mechanical elements as joints, gears, gaskets, brakes, roller bearings, clutches and more. Advanced computer methods allow the solution of complicated problems and require new methods for verification and modeling. A new method by Jäger (1995, 1998) "reduces" the friction problem to the normal problem, and therefore was called "reduced elastic friction model". There is also a correspondence between the conditions of Coulomb's law and the contact conditions, when two elastic bodies are in contact on the area C^*. An increase of the pressure p^* by Δp enlarges the contact area C^* to the size of C. The normal increment $\Delta p = p - p^*$ satisfies the contact condition for the relative displacement: $s_z = 0$ in C^*. For equal normal and tangential stress-displacement equations, the stick condition $s_x^* = 0$ is identical with the normal contact condition, assuming that C^* coincides with the stick area. Setting the traction $q = f\Delta p$ satisfies Coulomb's slip equation $q = fp$ in the slip zone $C - C^*$, with the coefficient of friction f and $p^* = 0$ outside of C^*. There are also two inequalities, (1) the traction q must be smaller than fp in the stick zone C^* and (2) the slip must

E-mail address: www@juergenjaeger.de (J. Jäger).

0020-7683/$ - see front matter © 2003 Elsevier Ltd. All rights reserved.
doi:10.1016/S0020-7683(03)00254-3

oppose the traction in the slip zone $C - C^*$. The stick inequality $q = f\Delta p = f(p - p^*) < fp$ is satisfied for positive pressure increments, and $\Delta p > 0$ is also the normal contact condition for a truncated punch with the flat base C^*. For equal stress-displacement equations, the normal and tangential displacements are proportional, which carries over to the slip, i.e. s_x is proportional to the normal relative approach $\Delta s_z = s_z - s_z^*$. The normal approach Δs_z opposes the normal pressure Δp, and the traction q opposes the slip s_x in the same way. It can be concluded that the mathematical model for friction is identical with the normal contact model, although it is physically different. This equivalence is independent of the mathematical form of the contact law. The integral of the traction gives the tangential force $F_x = f(F_z - F_z^*)$ as the difference of the slip force fF_z for the contact area and fF_z^* for the stick area. This equation can be used for the calculation of the virtual normal force $F_z^* = F_z - F_x/f$, which determines the stick area C^*.

The elastic friction principle cannot be regarded as a strict mathematical theorem, because physical applications require the omission of side effects, such as the coupling between tangential traction components of the classical Cattaneo–Mindlin model for paraboloidal surfaces. Some details of referred publications, which are necessary for the understanding of elastic properties, are included in the present manuscript, in order to make it more self-contained. The necessary assumptions and the proof of Coulomb's inequality were presented at the conference Pacam VII by Jäger (2002b). A summary of new solutions and a computer program for half-space problems, which is used below, can be found in a forthcoming book by Jäger (2003).

2. Formulation of the model

The basic assumptions of the reduced elastic friction model are

(1) Equal bodies of linear elastic materials in contact.
(2) Coulomb's rigid sliding law is used in a local form and assumes that the frictional traction is proportional to the pressure.
(3) The displacement–load equations are equal and uncoupled for all components.
(4) Advancing contact.
(5) Motion without rolling (no rotation around a tangential axis of contact).

The third assumption can be written

$$u_k = d_k f(x, y, \sigma_{zk}), \quad k \in \{x, y, z\}, \tag{1}$$

where u_k denotes the displacement components, σ_{zk} the components of the surface stress, d_k constant compliances, index k the coordinates x, y, z and $f(x, y, \sigma_{zk})$ an arbitrary function. Examples for the function $f(x, y, \sigma_{zk})$ are the integrals of line forces for half-planes (Jäger, 1997), constants for a plane strip (Jäger, 1999a), and a Winkler foundation (Jäger, 2000). Equal tangential compliances $d_x = d_y$, assure a constant direction of the displacements parallel to the tangential force, whereas the normal compliance d_z can be different.

The model of a rigid punch on a flat elastic plane is used as illustration of the contact and friction conditions. In the first step, the lower elastic plane is shifted upwards by the value ζ^* and a contact area C^* forms, as illustrated in Fig. 1, where the asterisk '*' characterizes values of step 1. We have the following conditions for the relative motion s_z^* of the lower elastic plane with respect to the rigid punch and the pressure $p^* = -\sigma_{zz}^*$

$$s_z^* = u_z^*(x) - \zeta^* \begin{cases} = -h(x) & \text{contact for } x \in C^*, \\ > -h(x) & \text{separation for } x \notin C^*, \end{cases} \tag{2}$$

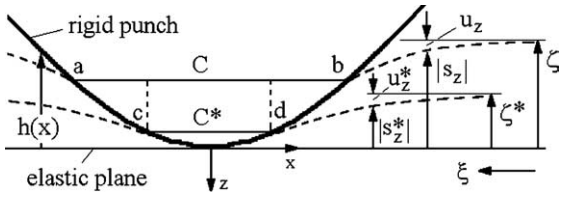

Fig. 1. Rigid punch in contact with an elastic plane.

$$p^* = -\sigma_{zz}^* \begin{cases} > 0 & \text{for } x \in C^*, \\ = 0 & \text{for } x \notin C^*, \end{cases} \tag{3}$$

with the gap $h(x)$ in undeformed contact. The relative motion $s_z^* < 0$ in Fig. 1 and the displacement u_z^* differ by the rigid body motion $-\zeta^*$ in Fig. 1.

In the next step, the compression is increased to the value ζ and a larger contact area C forms. The condition for contact and separation are the same as in Eqs. (2) and (3), when the asterisk is omitted for all variables, and Fig. 1 shows that points in the contact area C^* do not move relatively to the rigid punch. The contact condition (2) for the relative motion in the contact area must be $s_z(x) = -h(x) < s_z^*(x) < 0$ for $x \in C - C^*$ (Fig. 1), which will be used for the tangential solution, below. Assumption (4) assures that the contact area increases with the force, which implies that the pressure must not decrease in the whole contact area.

In the last step, a tangential displacement ξ is imposed on the elastic plane, and Coulomb's law requires that the tangential traction $\sigma_{zx} > 0$ in the slip zone of the elastic plane must be equal to the normal pressure multiplied with the coefficient of friction f (full slip traction)

$$\sigma_{zx} = f\ p \quad \text{in the slip area.} \tag{4}$$

Similar to the contact condition (2) in normal direction, the stick condition requires that the relative motion or slip $s_x = u_x - \xi$ must vanish in the stick zone, i.e. the displacement u_x must be constant. Each normal solution of (1) is also a tangential solution and the additional pressure $\Delta p = p - p^*$ causes a constant displacement of C^* in Fig. 1. Δp satisfies the stick condition when we assume that the stick area is identical with the smaller contact area C^*. Coulombs law in the slip zone can be satisfied by

$$\sigma_{zx} = f\Delta p = f(p - p^*), \quad x \in C. \tag{5}$$

There are also two side conditions of Coulomb's law: The slip s_x must be opposite to the traction σ_{zx} ($s_x < 0$ for $\sigma_{zx} > 0$) in the slip zone, and the traction in the stick zone must be smaller than the value for full slip fp. Since the displacements are unidirectional, the sign of the slip velocity $\mathrm{d}s_x/\mathrm{d}t$ of the conventional Coulomb law can be replaced with the sign of the integral s_x. Altogether we have the conditions

$$s_x = u_x - \xi \begin{cases} = 0, & x \in C^*, \\ < 0, & x \in C - C^*, \end{cases} \tag{6}$$

$$\sigma_{zx} = f(p - p^*) \begin{cases} = fp, & x \in C - C^*, \\ < fp, & x \in C^*. \end{cases} \tag{7}$$

The traction inequality (7) in the stick area C^* could only be violated for negative p^*, which would violate the contact condition (3), i.e. the traction inequality (7) is identical with the contact condition (2). Insertion of the traction (7) in the contact law (1) gives the relation

$$u_x = f\kappa(u_z - u_z^*) < 0, \quad \kappa = -d_x/d_z > 0. \tag{8}$$

Eq. (8) holds also for the rigid body terms ξ and ζ, using the contact and stick conditions (2) and (6) at the initial contact point. Insertion of (2) and (8) in (6) gives the condition

$$s_x = f\kappa(s_z - s_z^*) = f\kappa\Delta s_z < 0, \quad x \in C - C^*. \tag{9}$$

Eq. (9) is satisfied, because Fig. 1 shows that the absolute value $|s_z|$ for a point $x \in C - C^*$ in the slip area must be larger than $|s_z^*|$. Fig. 1 shows also that the slip condition (9) is identical with the condition of separation (2), because the surfaces of the punch and half-plane would overlap for $|s_z^*| > |s_z| = h(x)$.

The identity between Coulomb's inequalities and the normal contact conditions was questioned by Ciavarella (1999), who wrote that "*...there is no reason a priori to think that the inequalities in the normal contact* (*basically the condition for no overlap outside the contact area and positive pressure in the contact area*) *are connected at all with the inequalities of Coulomb's law, which Dr. Jäger seems to forget assuming a personal, reduced version of Coulomb's law* $q = fp$ *in the slip area*". The reason may be an error in Ciavarella's slip equation, where the rigid displacement ξ (δ in his notation) is missing, as discussed by Jäger (1999b). Ciavarella did not address the case of proportional loading and general loading scenarios, and Jäger's previous publications were omitted in his papers.

Integration of the stress (7) gives the equation for the forces. Eq. (8) for displacement $\xi = u_x(x_0)$ and $\zeta = u_z(x_0)$ at the initial contact point can be used to calculate the global force–displacement relation for constant normal forces and increasing tangential forces

$$F_x = f[F_z(\zeta) - F_z(\zeta^*)], \quad \zeta^* = \zeta - \xi/(f\kappa). \tag{10}$$

The equivalent normal displacement ζ^* can be calculated from the second equation (10) and inserted in the first equation for the force F_x. Numerically, the normal displacement can be applied in steps of ζ^* and the difference for the normal forces gives the tangential force. The stiffness factor κ can be determined by differentiation of Eq. (10)

$$\kappa = \frac{c_z}{c_x} = \frac{\mathrm{d}F_z(\zeta^*)/\mathrm{d}\zeta^*}{\mathrm{d}F_x(\xi)/\mathrm{d}\xi} = \frac{d_x}{-d_z}, \quad \zeta^* = \zeta - \xi/(f\kappa). \tag{11}$$

Eq. (11) allows the calculation of the stiffness ratio κ from numerical force displacement relations for constant ζ, e.g. for $\xi = 0$, $\zeta^* = \zeta$. The derivative of the force can be replaced by incremental differences. The theoretical relation $\kappa = -d_x/d_z$ in (11) follows after inversion of the displacement stress relation (1) for a special profile as a flat punch under complete adhesion: $\sigma_{zk} = f^{-1}(x, y, u_k)/d_k$. After integration, the displacement-force relation $\xi = d_x G(F_x)$ and $\zeta = d_z G(F_z)$ (with $\zeta = u_{z0}$, $\xi = u_{x0}$ and a function G) can be inserted in (11) and gives the right hand side $\kappa = -d_x/d_z$.

2.1. Proportional loading

Eqs. (10) and (11) can be used for proportional loading, where the force is applied at a constant angle β to the normal axis: $\mathrm{d}F_x = \tan\beta\,\mathrm{d}F_z$, $\mathrm{d}F_z > 0$. For $\tan\beta < f$, the increase of the tangential force $\mathrm{d}F_x$ is smaller than the value for sliding $\mathrm{d}F_x < f\,\mathrm{d}F_z$, and an infinitesimal slip area forms with $\zeta^* = \zeta - \mathrm{d}\xi/f\kappa \to \zeta$. Therefore, the virtual indentation of the stick area ζ^* can be replaced by ζ in (11) and we obtain

$$\mathrm{d}\xi = \frac{\mathrm{d}F_x(\xi)}{\mathrm{d}F_z(\zeta)}\kappa\,\mathrm{d}\zeta = \kappa\tan\beta\,\mathrm{d}\zeta, \quad \xi - \xi_0 = \kappa\tan\beta(\zeta - \zeta_0), \tag{12}$$

where the index "0" characterizes values at the beginning of proportional loading. The relation between the force components carries over to the traction $d\sigma_{zx} = \tan\beta\,\mathrm{d}p$, which can directly be integrated

$$\sigma_{zx} - \sigma_{zx0} = \tan\beta(p - p_0). \tag{13}$$

Relations (13) and (7) are identical for $\sigma_{zx0} = 0$, $p_0 = p^*$, with substitution of $\tan\beta$ for the friction coefficient f.

The derivation of this section can be extended to the three-dimensional case (even for multiple contact), when the plane case in Fig. 1 is considered as a sectional cut parallel to the tangential force, and all arguments are the same as in the plane case. Examples for the reduced friction model are presented at the end of this article, and others can be found in parallel publication (Jäger, 2002a).

3. General load histories

Load histories for thin strips were presented by Jäger (1999a), using the simple wire-brush model. This section shows that the same procedure can be used for other normal contact laws, when the assumptions of the reduced friction model are valid. General load histories can be thought as a superposition of loading increments of type (7), but it must be checked if the old and new slip zone overlap for two successive load increments. The normal and tangential component of each increment are applied in two steps. When $\Delta\zeta_k$ increases, the normal component $\Delta\zeta_k$ is applied before the tangential component $\Delta\xi_k$. In order to simplify the algorithm, the order of application is changed for decreasing $\Delta\zeta_k < 0$, where the tangential component $\Delta\xi_k$ must be applied first, and the normal component after that. This procedure avoids that normal unloading reduces the previous stick region in the special case when the tangential load increment is opposite to the previous increment. For a reverse tangential load increment, the old slip zone sticks at the beginning, whereas normal unloading, on the other hand, increases the slip zone and decreases the normal pressure.

An example for a positive increment Δq_1 and negative Δq_2 is illustrated in Figs. 2 and 3 and others were published by Jäger (1996, 1998) for paraboloidal surfaces and plane elasticity. The general algorithm requires the introduction of the following three contact regimes: no overlapping (n.o.), partial

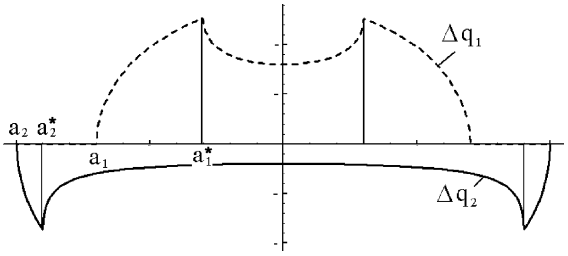

Fig. 2. No overlapping for $k = 2$, $f_1 = -f_2 = f$.

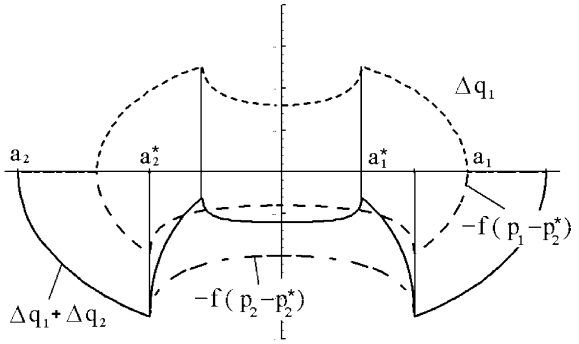

Fig. 3. Partial overlapping $k = 2$, $f_1 = -f_2 = f$.

overlapping (p.o.), and complete overlapping of the old and new slip zone. The mathematical formula for the tangential traction increment Δq_k can be written in the form

$$\Delta q_k = \begin{cases} f_k(p_k - p_k^*) & \text{for n.o.,} \\ f_k(p_k - p_k^*) - f_{k-1}(p_{k-1} - p_k^*) & \text{for p.o.,} \end{cases} \tag{14}$$

$$\Delta \xi_k = \begin{cases} f_k \kappa(\zeta_k - \zeta_k^*) & \text{for n.o.,} \\ f_k \kappa(\zeta_k - \zeta_k^*) - f_{k-1}\kappa(\zeta_{k-1} - \zeta_k^*) & \text{for p.o.,} \end{cases} \tag{15}$$

with $p_k = p(a_k)$, $p_k^* = p(a_k^*)$, $f_k = \pm f$ and the superscript '*' for values of the stick area. The pressure can also be written as a function of the virtual indentation ζ, i.e $p = p(\zeta)$, $p^* = p(\zeta^*)$. Further, the formula for the tangential force can be obtained by substitution of F_x for q and F_z for p in (15), because integration gives the force. In the first line of (14), the contact regime of n.o. takes place, where the old and new slip zone do not overlap, and we have $a_k^* > a_{k-1}$ ($a_2^* > a_1$ in Fig. 2). This solution was explained in the section on tangential contact above. For $a_k^* < a_{k-1}$, p.o. takes place ($a_1^* < a_2^* < a_1$, in Fig. 3). Here, the overlapping part of the old and new slip zone must first be made traction free by the second expression in square brackets, before a traction distribution can be superposed, which satisfies Coulomb's law. Finally, for $a_k^* < a_{k-1}^*$, we have complete overlapping, and the old slip zone of step $k-1$ is erased.

The general algorithm for displacement controlled loading begins with the test of the stick condition for a load increment k and consists of the following three steps:

1. Test the stick condition $|\Delta \xi_k| < f\kappa\Delta\zeta_k$. When it is satisfied, we have n.o. and Eq. (14) gives the corresponding traction increment for n.o. The solution is found.
2. $|\Delta \xi_k| \geqslant f\kappa\Delta\zeta_k$. A new slip zone forms and we have either partial or complete overlapping of the old slip region. The virtual displacement ζ_k^* can be calculated from Eq. (15) for p.o., when the displacement increments, $\Delta\xi_k$ and $\Delta\zeta_k$ are given. For $\zeta_k^* > \zeta_{k-1}^*$ only a part of the old slip zone is erased by the new slip traction and the traction increments are given by Eqs. (14) for p.o. The solution is found.
3. The stick condition $|\Delta \xi_k| < f\kappa\Delta\zeta_k$ and the condition for p.o. $\zeta_k^* > \zeta_{k-1}^*$ are violated and the new slip region overlaps the old slip zone completely. Apply the old and new increment $\Delta\xi_k + \Delta\xi_{k-1}$ in one step and repeat steps 1–3.

This algorithm must be successively repeated for all steps of the load history, starting with the first step. An equivalent load history remains, where the contact regimes of complete overlapping have been eliminated. The force is the integral over the traction. A similar algorithm was published in Jäger (1996), for three-dimensional loading with oblique load increments.

4. Comparison with FEM

A FEM solution for a flat rounded punch was compared with an analytical solution at Contact Mechanics V by Jäger (2001). The model and the interior stress field for frictional loading in Figs. 4 and 5 illustrate the agreement between both solutions. Additional information can be found in the mentioned publication. The program ANSYS 5.5 was used with rigid elements TARGE169 for the rigid punch with the semi-axis $b = 5$ mm of a flat region and a rounding with radius $R_c = 80$ mm. A circular region of the half-plane was modeled with 2-D elements PLANE42 and was fixed radially at $R_G = 50$ mm. The x-axis of the half-plane represented the contact surface and consisted of CONTA171 elements, which were associated with the target elements. The half-plane had a modulus of Elasticity $E = 1000$ N/mm^2, Poisson's ratio was $\nu = 0.4999 \approx 0.5$ and the coefficient of friction $f = 0.5$. The normal force was applied in steps 1–3 with the values $a = \{5.4, 5.8, 6.2\}$ of the contact semi-axis. Four increments were used for each step. After normal loading,

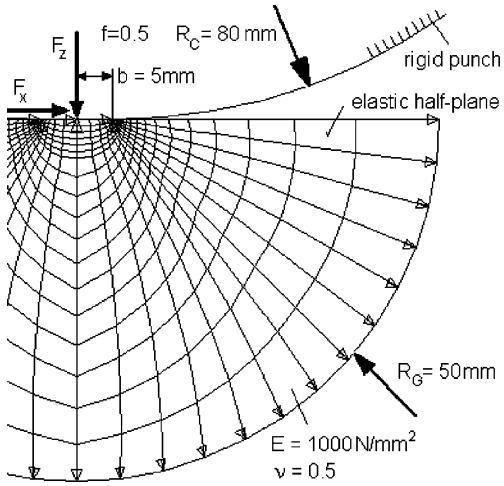

Fig. 4. FEM model of a punch on a plane.

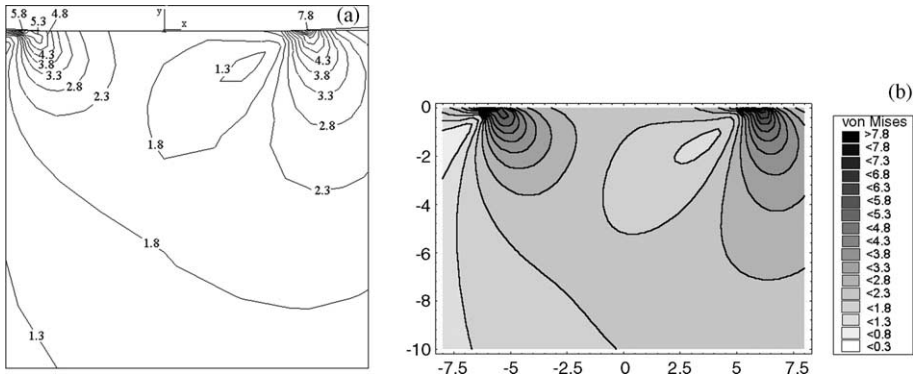

Fig. 5. FEM solution on the left (a) and analytical result on the right (b) hand side.

a tangential force was applied in steps 4–6, with the values $a^* = \{5.8, 5.4, 0\}$ for the semi-axis of the stick area. With these values, the tangential traction can be calculated from Eq. (7) with $p = p(a)$ and $p^* = p(a^*)$.

A closed analytical solution for Muskhellishvili's potential for the interior stress filed was calculated with a superposition method by Jäger (2001). Fig. 5 compares results of step 5 in the regime of partial slip ($a^* = 5.4$) for a FEM model (left hand side) and an analytical solution. The maximum and the form of the contours are the same for both methods, but the discrete FEM mesh produces some corners in the contours. More information on the derivation of the analytical solution of this model can be found in the mentioned paper by Jäger (2001), and it was shown by Jäger (2002a) that the reduced friction model can also be used for small dissimilarity effects. Another example for dissimilar contact is analyzed in the next section.

5. Torus

An example of two horizontal elastic half-spaces in contact on a circular ring, with a radius $R_m = 0.5$ mm of the undeformed contact circle, was calculated numerically using a program by Jäger (1992). For small

displacements, the surface profile can be approximated by a parabolic rounding at the initial contact line, of the form $r^2/(2R_c)$, with $R_c = 1$ mm in this example. For small displacements, the force–displacement curve is almost linear, and the friction hysteresis of tangential loading very small. Therefore, as illustration of the reduced friction model, a relatively large normal displacement increment of $\Delta\zeta = 0.1$ mm was applied in 10 steps. In practical problems, the stresses and displacements must be much smaller, and the reduced friction model gives even better approximations as in the figures below.

A characteristic parameter for the dissimilarity effect is the dissimilarity parameter γ (Dundurs' constant, Dundurs, 1975)

$$\gamma = \frac{\frac{1-2\nu_1}{2G_1} - \frac{1-2\nu_2}{2G_2}}{\frac{1-\nu_1}{G_1} + \frac{1-\nu_2}{G_2}} \leqslant 0.5, \tag{16}$$

where the index signifies body 1 or 2. γ describes the coupling effect between the normal and tangential components, which was neglected in Eq. (1). γ increases with decreasing Poisson ratios ν and has a value of $\gamma = 0.29$ for this example. For most metals, Poisson's ratio has a value of $\nu \approx 0.2$–0.3 (Beryllium excepted with $\nu \approx 0.03$). An improved parameter γ/f was used by Spence (1973) to classify the size of the stick area for normal loading of self-similar profiles. He found that the slip area increases with γ/f. A numerical calculation of tangential impact of dissimilar spheres (Jäger, 1992) shows that the coefficient of restitution for the tangential velocity changes with γ/f, but a relatively low friction coefficient is necessary for significant differences compared with similar materials. The material dissimilarity has only a small influence on the normal velocity of central impact, especially for low friction.

The dissimilarity parameter for standard structural materials in contact is very small. Steel ($\nu_2 = 0.3$, $G_2 = 83{,}077$ N/mm^2) in contact with Aluminum ($\nu_1 = 0.33$, $G_1 = 22{,}556$ N/mm^2) was selected for this example, which may be regarded as a worst case for dissimilarity. The equivalent similar problem of uncoupled half-spaces requires the material parameters $\nu_1 = \nu_2 = 0.5$, $G_1 = G_2 = 26{,}227$ N/mm^2. Since the dissimilarity effect increases with falling coefficients of friction, a small coefficient of friction $f_{stat} = f_{kin} = 0.2$ was selected. After normal loading, the tangential displacement $\Delta\xi_1 = 0.02$ mm was applied in 11 steps, followed by unloading $\Delta\xi_2 = -0.02$ mm in 22 steps. The stiffness factor for similar material is defined as $\kappa = 0.5^*(2-\nu)/(1-\nu) = 1.5$. For dissimilar material, $\kappa = 1.26$ was determined numerically using Eq. (11), as the ratio $\Delta F_z/\Delta\zeta$ for the last increment of the normal loading path and $\Delta F_x/\Delta\xi$ for the first increment of tangential loading.

Fig. 6 shows the tangential force–displacement curves for similar (solid line) and dissimilar materials (broken line). The dimension of the force is N and of the displacement mm. The discrepancy between the dissimilar solution and the corresponding reduced friction model (circles) is maximum for the first

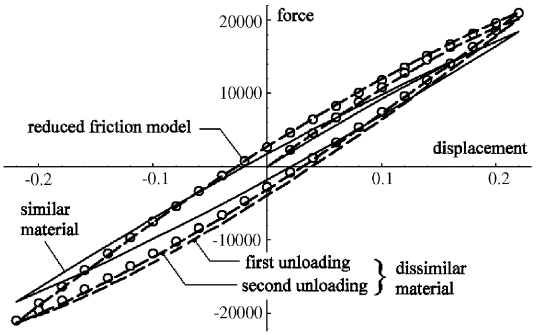

Fig. 6. The reduced friction model (circles) compared with numerical results for dissimilar material (broken line).

unloading curve. It can be concluded that the reduced friction model gives a good approximation for the force–displacement curves of the dissimilar problem, especially for repeated unloading.

Fig. 7 illustrates the asymmetric pressure distribution and Fig. 8 the tangential tractions for initial tangential loading of similar material. The tractions values in Fig. 7 are scattered for small values of the radius, due to the coupling between the tangential traction components of similar material. The solution of the reduced friction model from Eq. (5) is presented with a broken line for the values $\xi = 0.06, 0.12, 0.18$. As example, the values for the load increment $\xi = 0.06$ are: $\zeta^* = \zeta - \xi/f\kappa = 0.8$, $\zeta = 1$, $f = 0.2$, $\kappa = 1.5$, so that the calculated values of the normal loading can be inserted in (5) $q = f(p(\zeta) - p(\zeta^*)) = f(p(1) - p(0.8))$, as the pressure difference for $\zeta = 1$ and 0.8.

Finally, the asymmetric stick and slip areas are shown in Fig. 9 for dissimilar materials. The present example is useful for the illustration of Eqs. (14) and (15). The force displacement relation of the normal solution $F_z = F_z(\zeta)$ is used for the reduced friction model. The normal increment was applied in 10 increments $\Delta\zeta = 0.1$ and the resulting force F_{zi} for increment i can be interpolated. The formulas for the first loading in tangential direction in Fig. 6 are given by (14) and (15) for n.o.

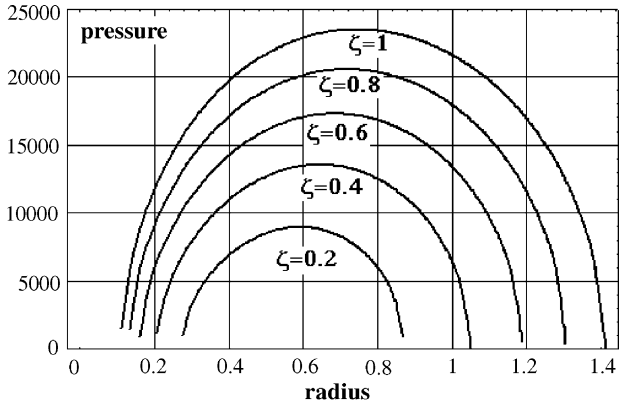

Fig. 7. The pressure p in N/mm^2 for similar materials calculated with 80×80 points in the potential contact area.

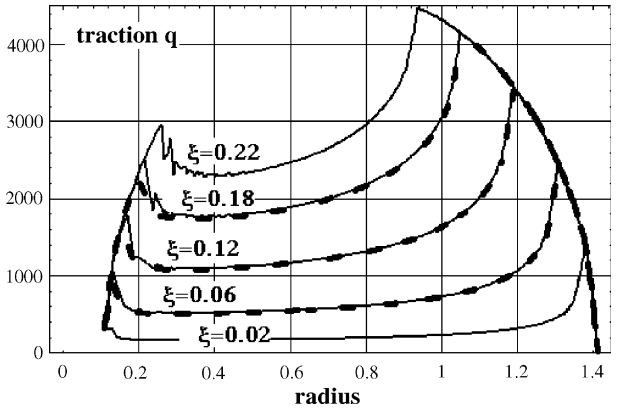

Fig. 8. Tangential traction q in N/mm^2 for initial tangential loading of the numerical solution (solid line) for similar material and the reduced friction model (broken line).

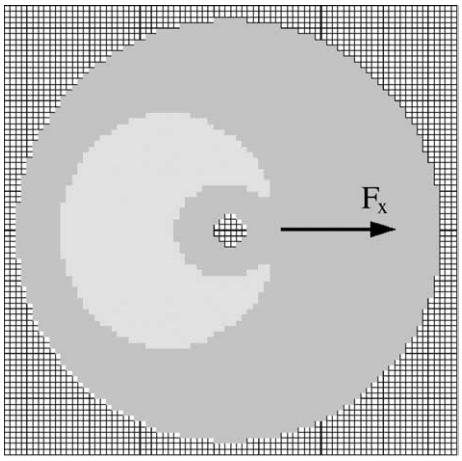

Fig. 9. Stick area (light gray) and slip area (dark gray) for dissimilar material (80×80 points, $\xi = 0.2$, initial tangential loading).

$$\begin{aligned} &\Delta\xi_1 = \xi_1 = f_1\kappa(\zeta_1 - \zeta_1^*), \quad \Delta F_{x1} = F_{x1} = f_1(F_{z1} - F_{z1}^*), \\ &\zeta_1^* = \zeta_1 - \xi_1/f_1\kappa \end{aligned} \tag{17}$$

The first Eq. (17) gives ζ_1^* and determines $F_{z1}^* = F_z(\zeta_1^*)$

$$F_{x1}(\xi_1) = f_1F_z(\zeta_1) - f_1F_z(\zeta_1 - \xi_1/f_1\kappa), \tag{18}$$

where the force F_z is written as a function of ζ. In this example the normal displacements ζ_1 is constant, but the formula (18) holds also for decreasing ζ_1. At the point $\xi_1 = 0.22$, the tangential displacement is decreased by negative $\Delta\xi_2$. Reverse slip takes place with p.o. in Eqs. (14) and (15). The normal displacement is constant $\zeta_1 = \zeta_2$ and slip is opposite $f_2 = -f_1$.

$$\begin{aligned} &\Delta\xi_2 = f_2\kappa(\zeta_2 - \zeta_2^*) - f_1\kappa(\zeta_1 - \zeta_2^*) = -2f_1\kappa(\zeta_1 - \zeta_2^*), \\ &\Delta F_{x2}(\xi_2) = -2f_1(F_{z1} - F_{z2}^*). \end{aligned} \tag{19}$$

Summation of the increments (18) and (19) gives $\xi_2 = \Delta\xi_1 + \Delta\xi_2$ which can be solved for ζ_2^*

$$\zeta_2^* = \zeta_1 + \frac{\xi_2 - \xi_1}{2f_1\kappa}. \tag{20}$$

Summation of (18) and (19) gives the tangential force $F_{x2} = \Delta F_{x1} + \Delta F_{x2}$ for unloading

$$F_{x2}(\xi_2) = -f_1F_z(\zeta_1) - f_1F_z\left(\zeta_1 - \frac{\xi_1}{f_1\kappa}\right) + 2f_1F_z\left(\zeta_1 + \frac{\xi_2 - \xi_1}{2f_1\kappa}\right). \tag{21}$$

The result for the reloading curve F_{x3} can be obtained by substitution of index 3 for 2, $-f_1$ for f_1 and $\xi_1 = -0.22$. This example illustrates the advantage of the numerical evaluation compared with the cumbersome manual calculation of Eqs. (14) and (15).

6. Conclusion

Fundamental properties of the elastic friction model have been presented for general three-dimensional contact laws, and it has been shown that Coulomb's inequalities are identical with the contact inequalities.

New methods for proportional and general loading scenarios have been presented, in form of a generalization of special earlier solutions for thin strips and paraboloidal surfaces. It has been shown in the paper that the frictionless normal load–displacement curve is sufficient for the determination of the frictional force–displacement relation. This can save much computing time, because the friction solution is non-linear and time-consuming. Future applications of this model are fretting and wear of machine elements, brakes, gears, fasteners, and impact problems with friction. It is possible to remove the restrictions of the reduced friction model, and to develop corrections for non-elastic materials. The elastic friction principle can also be employed in the field of plasticity as a model for isotropic and kinematic hardening. A FEM example for a flat rounded punch has been presented at the end of the article and the dissimilarity effect was illustrated for annular contact. A BEM program was used for the solution of a contact area with 3600 elements, which is much larger than typical contact solutions with FEM models. It was shown that the force–displacement relation of the reduced friction model can be used as approximation for dissimilar materials, although the basic assumption of equal material in contact is violated. An explanation may be that the local redistribution of the stress has a small influence on the global behavior.

References

Ciavarella, M., 1999. Author's closure. J. Appl. Mech. 66, 1049–1050.

Dundurs, J., 1975. Properties of elastic bodies in contact. In: de Pater, A.D., Kalker, J.J. (Eds.), Mechanics of Contact Between Deformable Bodies. Delft University Press, Delft, The Netherlands, pp. 54–66.

Jäger, J., 1992. Elastic impact with friction, Thesis, Dep. Maths. and Infs., Delft University, Delft, The Netherlands.

Jäger, J., 1995. Axi-symmetric bodies of equal material in contact under torsion or shift. Arch. Appl. Mech. 65 (7), 478–487.

Jäger, J., 1996. Stepwise loading of half-spaces in elliptical contact. J Appl. Mech. 63, 766–773.

Jäger, J., 1997. Half-planes without coupling under contact loading. Arch. Appl. Mech. 67, 247–259.

Jäger, J., 1998. A new principle in contact mechanics. J. Tribology 120, 677–683.

Jäger, J., 1999a. A generalization of Cattaneo–Mindlin for thin strips. Arch. Appl. Mech. 66, 1034–1037.

Jäger, J., 1999b. Discussion of tangential loading of general three-dimensional contacts. J. Appl. Mech 66, 1048–1049.

Jäger, J., 2000. Conditions for the generalization of Cattaneo–Mindlin. Z. Angew. Math. Mech. 80, S383–S384.

Jäger, J., 2001. New analytical solutions for a flat rounded punch compared with FEM. In: Conference Contact Mechanics V, Wessex Institute of Technology. WIT press, Southampton, pp. 307–316.

Jäger, J., 2002a. Fundamentals of a reduced elastic friction model. Int. J. Problems Nonlinear Anal. Eng. Sys., Kazan 8 (2), 1–10.

Jäger, 2002b. Properties of equal bodies in contact with friction. In: Kittl, P., Diaz, G., Mook, D., Geer, J. (Eds.), Proc. PACAMVII, Universidad de la Frontera, Temuco, pp. 121–124.

Jäger, J., 2003. New solutions in contact mechanics. Wessex Institute of Technology, WIT Press, Southampton.

Spence, A., 1973. An Eigenvalue problem for elastic contact with finite friction. Proc. Camb. Phil. Soc. 73, 249–268.